The NuMoon Experiment: Preliminary results and upper limits on UHE particles.

G. K. Krampah,[a,*] **S. Buitink,**[a,b] **J. Bhavani,**[a,b] **M. Desmet,**[a] **A. Corstanje,**[a,b]
H. Falcke,[b,c,d] **B. M. Hare,**[e] **J. R. Hörandel,**[a,b,c] **T. Huege,**[a,f] **N. Karasthatis,**[f]
K. Mulrey,[b] **P. Mitra,**[a] **A. Nelles,**[g,h] **K. Nivedita,**[b] **H. Pandya,**[a] **J. P. Rachen,**[a]
O. Scholten,[i] **S. ter Veen,**[b,d] **S. Thoudam,**[j] **T. N. G. Trinh**[k] **and T. Winchen**[l]

[a]*Astrophysical Institute, Vrije Universiteit Brussel, Pleinlaan 2, 1050 Brussels, Belgium.*

[b]*Department of Astrophysics/IMAPP, Radboud University, P.O. Box 9010, 6500 GL Nijmegen, The Netherlands.*

[c]*Nikhef, Science Park 105, 1098 XG Amsterdam, The Netherlands.*

[d]*Netherlands Institute of Radio Astronomy (ASTRON), Postbus 2, 7990 AA Dwingeloo, The Netherlands.*

[e]*University of Groningen, Kapteyn Astronomical Institute, Groningen, 9747 AD, Netherlands.*

[f]*Institut für Kernphysik, Karlsruhe Institute of Technology (KIT), P.O. Box 3640, 76021, Karlsruhe, Germany.*

[g]*DESY, Platanenallee 6, 15738 Zeuthen, Germany.*

[h]*ECAP, Friedrich-Alexander-University, Erlangen-Nürnberg, 91058 Erlangen, Germany.*

[i]*Interuniversity Institute for High-Energy, Vrije Universiteit Brussel, Pleinlaan 2, 1050 Brussels, Belgium.*

[j]*Department of Physics, Khalifa University, P.O. Box 127788, Abu Dhabi, United Arab Emirates.*

[k]*Department of Physics, School of Education, Can Tho University Campus II, 3/2 Street, Ninh Kieu District, Can Tho City, Vietnam.*

[l]*Max-Planck-Institut für Radioastronomie, Auf dem Hügel 69, 53121 Bonn.*

[m]*Department of Physics, Khalifa University, P.O. Box 127788, Abu Dhabi, United Arab Emirates.*

E-mail: gkrampah@vub.be

*Speaker

The main goal of the NuMoon experiment is study ultra-high energy cosmic rays and neutrinos interacting with the Moon using ground-based radio telescopes. Ultra-high energy (UHE) particles interacting with the Moon produce particle showers in the regolith. Due to charge asymmetry in the shower front, a short broadband coherent burst of radio emission is produced - via a phenomenon referred to as the Askaryan effect. With ground based radio telescopes, such pulses can be searched for. The LOw Frequency ARray (LOFAR) - a radio observatory located in the Netherlands - is currently the largest radio array operating at frequencies between $110 - 190$ MHz; an optimal frequency range for Lunar signal search. A pulse search on the near-surface of the Moon is carried out. This requires a proper understanding of the background noise and other factors (like the ionosphere) that could have an adverse effect on the signal. In this contribution, we discuss results from first Lunar observations with LOFAR and the development of a trigger algorithm for future observations. Results from a detailed Monte-Carlo (MC) simulation of the effective lunar aperture for UHE particles and the expected sensitivity to the UHE particle flux are shown.

1. Introduction

Cosmic rays are highly energetic protons and nuclei and have been observed up to energies of almost 10^{20} eV. The nature of the observed cutoff in the spectrum is still uncertain. While it is possible that it represents the maximum energy to which cosmic rays can be accelerated in their sources, it also coincides with the GZK energy. Above the GZK energy, cosmic particles lose their energy via interactions with the 2.7 K Cosmic Microwave Background (CMB) photons as well as other radio backgrounds, over distances of the order of tens of megaparsecs. The observed energy cut-off could thus be the result of the lack of sources at close proximity. Detailed observation of the shape of the energy spectrum near the cutoff will allow us to distinguish between these scenarios and learn more about the sources of cosmic rays and their acceleration mechanisms.

Detecting neutrinos may also play a significant role in solving the mystery of origin of cosmic rays as they are not affected by (inter-)galactic magnetic fields. They are produced when energetic cosmic rays interact with matter and radiation on their path to Earth or in their sources. Ultra-high energy (UHE) protons scattering off the CMB produce π^+ which decays to produce neutrinos. These are called GZK neutrinos. Alternatively, neutrinos at these (or higher) energies could be produced in top-down models that predict neutrinos coming from the decay of supermassive particles. These supermassive particles are topological defects or magnetic monopoles that could be produced in the early universe during the symmetry-breaking phase transitions embedded in the grand unified theories [1–3]. These exotic models predict various fluxes of UHE cosmic neutrinos, whose detection would provide an important test of models for the evolution of the Universe.

The low flux of UHE particles around the energy cutoff requires that we build very large detector arrays. In the 1960s Askaryan proposed to use the Moon as a detector volume [4], though the initial assumption was to put detectors on the Lunar surface. Later, Dagkesamanskii and Zheleznykh [5] suggested to use Earth-based radio telescopes to search for lunar pulses produced by UHE cosmic rays or neutrinos interacting with the Moon. The near-surface of the Moon which is about 19 million km^2 implies that even for a flux as low as one particle per km^2 per century (at 10^{20} eV) culminates into an impact every 3 minutes. The rather large average Earth-Moon distance (of $\approx 3.88 \times 10^8$ m) puts a very high energy threshold for particle detection. The Moon is opaque to UHE neutrinos and hence interact with $\approx 20\%$ of their initial energy going into a detectable hadronic shower. For charged current interaction, the remaining 80% of the energy goes into creating an electromagnetic shower which is undetectable due the LPM effect [6]. The cascade in the Moon develop a negative charge excess propagating at a greater phase velocity than light in the Moon. This produces a radio emission which is intense at the Cherenkov angle. At wavelengths (i.e. lower frequencies) greater than the shower dimension, the emission is coherent over a larger angular width around the Cherenkov angle. This is the reason why the NuMoon experiment uses a low frequency band. At lower frequencies, as opposed to higher frequencies, a larger fraction of the Lunar surface falls within the detection volume as a significant fraction of the emanating radiation can escape total internal reflection. In the instance of no detection, upper limit can be put on the flux of the UHE neutrino but this requires an accurate knowledge of the aperture. In the contribution, we discuss a Monte Carlo simulation of the aperture and some preliminary results from Lunar observation with LOFAR.

2. Monte-Carlo Simulation of the Effective Lunar Aperture

The following assumptions were made in this simulation: all neutrinos are treated equally (i.e. all flavours produce similar hadronic showers and signals), regolith depth of 1 km with a fixed refractive index, 1.73 (implies all inhomogeneities are ignored), emissions are only coming from hadronic showers. The fraction of the primary neutrino energy that initiates a hadronic shower is referred to as the inelasticity and whose values are sampled from a distribution with a mean value of 20%. In the event generation, we simulate neutrinos from the same direction while randomizing the location of Earth (i.e. in effect, we are calculating which part of the lunar sky receives a detectable signal. This translates to simulating many neutrino arrival directions) as against what happens in reality, where the Earth's position is fixed, and the neutrinos arrive from random directions. The reason for this choice is that, there is almost no chance that an emitted ray from the Moon will hit a detector at Earth (at LOFAR) because of small projected solid angle of the LOFAR observatory and secondly, physics works in reverse. For each simulated neutrino, a penetration depth and impact parameter are sampled from a distribution. The penetration depth which is sampled from an exponential distribution (which depends on the neutrino mean-free-path and gives different weights to the neutrinos) is the emission point. With these two parameters, we move to a another geometry where we calculate the depth or height below the local surface. At the emission point, a number of n rays are generated uniformly on a hemisphere with each ray having associated with it a solid angle ($2\pi/n$ inside the regolith), a polarization and an electric field strength taken from [7]. The rays are propagated to the surface, taking into account attenuation losses [8], total internal reflection and refraction. At the surface, the total field is separated into parallel and perpendicular polarization and the appropriate modified Fresnel transmission coefficient (due to divergence after refraction) applied. For each transmitted signal above the trigger threshold, the appropriate modified solid angle (due to divergence after refraction) is computed, summed up, and normalize by 2π (since the transmitted rays fill a hemisphere). This gives the detection probability for that particular neutrino. These probabilities are calculated for a number of neutrinos with the same energy to obtain an averaged probability for that particular energy. With the averaged probability, the effective lunar aperture for neutrinos of a particular energy is computed. By summing the transmitted solid angles of the rays, we are in effect calculating the fraction of the sky that receives a detectable signal. Lunar surface topography affects the detection probability of interacting neutrinos with the Moon. The surface topography can be classified as either small-scale, medium-scale and large-scale roughness. In the contribution, we only considered the large scale roughness where the surface slope remain constant over the entire length of the shower. The root-mean-square (rms) slope is given as [9]: $\tan s_{rms} = 0.29(\lambda[\text{cm}])^{-0.22} = 0.14(\nu[\text{GHz}])^{0.22}$, where λ and ν are wavelength and frequency respectively. This equations shows that the surface is rougher at higher frequencies. The adirectional slope distribution is similar to Rayleigh distribution which is obtained by summing two Gaussian (or unidirectional) distribution of slopes in quadrature (i.e. along the x and y axis) [10]. The Gaussian distribution of slope has mean 0 and standard deviation, $\tan s_{\text{rms}}$ and then taking the tan inverse.

The results of the simulation were compared with an analytic parameterization [11] and shown in figure 1. In this figure, considered an instance where the lunar surface is smooth in both simulation (in red) and analytic parameterization (magenta) and the results are in good agreement. It should be noted that, a constant transmission coefficient, 0.6 and inelasticity, 0.2 are used for this figure. A
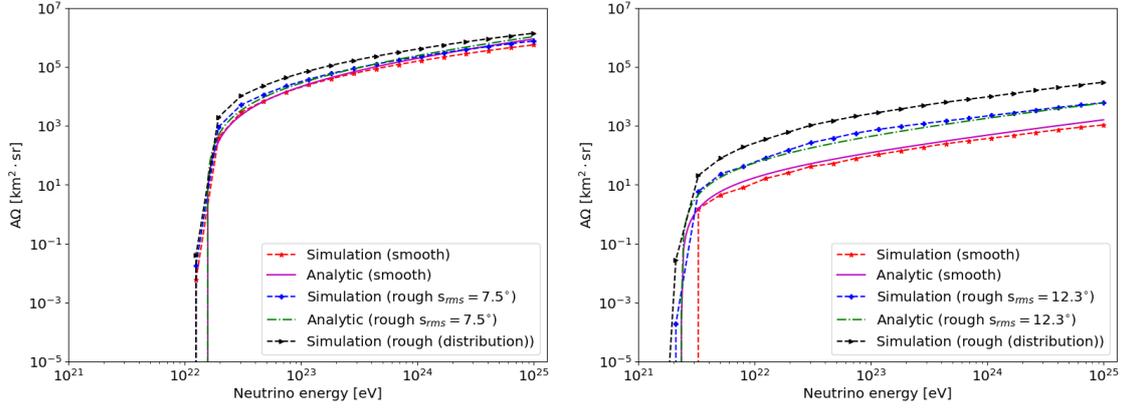
Figure 1: Plot of neutrino aperture versus energy assuming a constant inelasticity, 0.2 and transmission coefficient, 0.6 and taking into account surface roughness. Left: 150 MHz, right: 1.50 GHz.

large scale roughness (i.e. slope remains constant across the full length of the shower) of the lunar surface is also considered in both simulation (in blue) and analytic parameterization (in green) where each event see the same rms surface slope, s_{rms}. Both simulation and analytic expression are again in good agreement except for a threshold energy shift at high frequencies. Roughness as can be seen, enhances the detection probability particularly from downward neutrinos which will otherwise not be detected due to total internal reflection. A more realistic lunar surface topography is considered in the simulation where the surface slopes are sampled from a Rayleigh distribution (in black) and as can be seen, the detection probability is further enhanced even for lower frequencies. This is because surface roughness enhancement becomes particularly important when the slope exceeds the Cherenkov cone width. In summary, surface roughness enhances detection at all frequencies but more effective at higher frequencies where the lunar surface appears rougher.

The simulation is repeated as before but this time, the transmission coefficient is properly calculated and the inelasticity sampled from a realistic distribution. The net effect of these two decreased the energy threshold allowing for the detection of lower energy neutrinos. Thus, these two parameters determines the minimum detectable neutrino energy.

3. Results from Preliminary Lunar Observation with LOFAR and Trigger Algorithm

Observations were carried out on the 29$^{\text{th}}$ November, 2020 at 22 UTC for one minute using 6 half LOFAR core stations in the Netherlands. All beams were directed at the Moon located at 18.69° DEC and 61.28° RA. The 6 stations used are: 'CS003HBA0', 'CS013HBA0', 'CS030HBA0','CS031HBA0', 'CS301HBA0' and 'CS401HBA0'. The station data is RFI filtered, de-dispersed and beam-formed to form 49 tied-array beams each pointing at a small region of the lunar surface. This data is analyzed to understand the RFI background and to suppress RFI that have escaped the initial RFI algorithm. To this end, a unit-less parameter, P_5:

$$P_5 = \frac{\sum_{5\text{samples}} P_x}{\langle \sum_{5\text{samples}} P_x \rangle} + \frac{\sum_{5\text{samples}} P_y}{\langle \sum_{5\text{samples}} P_y \rangle} \tag{1}$$

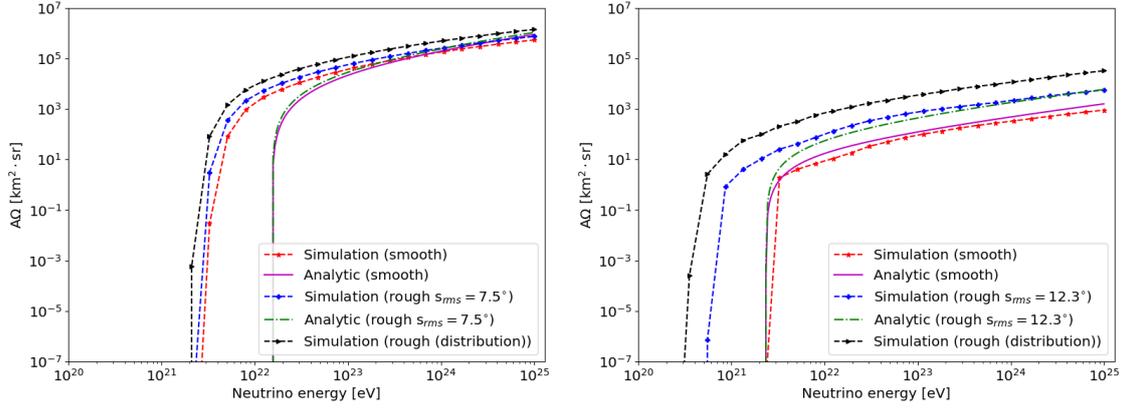

Figure 2: Plot of neutrino aperture versus energy with realistic distribution of the inelasticity, calculated transmission coefficient and large scale surface roughness. Left: 150 MHz, right 1.50 GHz.

is defined for all 49 tied-array beams due to the measured uncertainty in slant total electron content (*STEC*) of the ionosphere which causes the pulse width to increase and hence the choice of 5 samples/bins over which the power is spread for a nyquist sampled band-limited pulse. Some sources of background are as follows: strong horizon pulse (which show up as consecutive pulses in all 49 tied-array beams) and a local pulse at a single station (will be present in 49 beams). Askaryan-like pulses will be seen in all station beams and will appear as a strong pulse in some tied-array beams (due to beam side-lobes) and not all tied-array beams. Based on these, a trigger algorithm is designed which depends on the P_5 values. The trigger parameters are:

- the standard deviation, σ of the maximum P_5 values of the 49 tied array beams

- $n40$: number of maximum P_5 values from the 49 beams in the 40th percentile

Figure 4 is a plot of the $n40$ versus standard deviation from both simulation and data. We simulate signals from both the horizon and from random positions on the surface of the Moon. Askaryan-like pulses are expected in the lower right corner of these plots as demonstrated in the simulation. Using this plot, we classify events as either RFI-like or signal-like and studied them in further details by looking at all the 49 tied-array beams and the individual station beams. Figure 3 (left) is distribution of P_5 values for data and pure Gaussian noise. The filtered or triggered data are those for which $n40 < 20$ and standard deviation, $\sigma > 2$. The highest energy signal-like events in the data upon further studies are not real Askaryan-like events as we seen strong local pulse at some stations. Given that no Askaryan pulses were found for this initial observation (i.e. only 40 seconds of 1 minute data is analysed for this work), an upper limit (at 90% confidence level and assuming Poisson counting statistics) [12]:

$$F(E, t) < 2.3 \frac{E}{t A_e(E)} \tag{2}$$

can be put on the UHE neutrino flux as shown in figure 3 (right). $A_e(E)$ is the energy dependent effective aperture, and t is the effective observing time. Shown in this figure is the upper limit for 40 seconds of observed data from LOFAR using aperture calculation described above. We
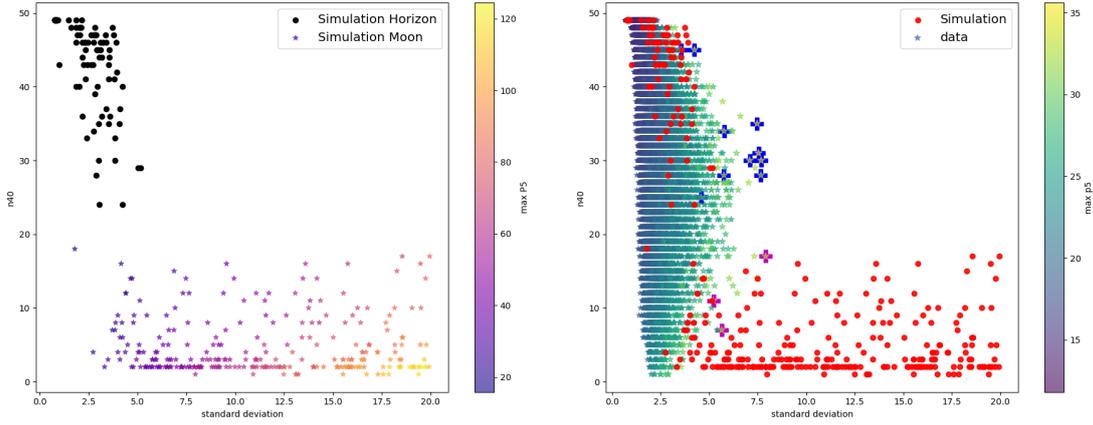
Figure 3: Plot of *n*40 versus standard deviation. Left: Based on simulation only, right: Both simulation and data. Plus (+) markers in blue are RFI-like events and purple are signal-like events.
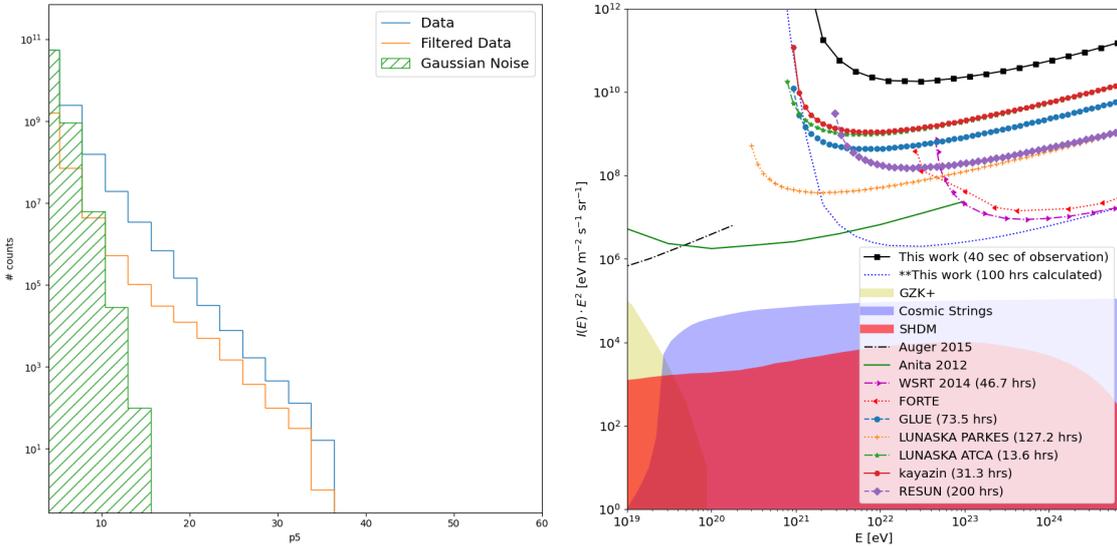

Figure 4: Plot of *n*40 versus standard deviation. Left: Based on simulation only, right: Both simulation and data. Plus (+) markers in blue are RFI-like events and purple are signal-like events.

also calculated an upper limit for an extrapolated time of 100 hours of observation with no detection. Also, upper limits from other experiments are shown except that the results from "GLUE", "LUNASKA PARKES", "LUNASKA ATCA", "kayazin" and "RESUN" are based on analytical parametrization [11].

4. Summary and Outlook

We have calculated the effective lunar aperture in which we took into account the lunar surface roughness on a large scale. Effect of small scale roughness on the aperture will be discussed in a later paper. We have presented the preliminary results from one minute of observing time, discussed the triggering the techniques and established an upper limit on the UHE neutrino flux. Longer observing

hours and including more LOFAR stations in an observing run give an increased sensitivity for detection or provide the best upper limit to constrain source models for UHE neutrinos.

References

[1] P. Bhattacharjee and N.C. Rana, *Ultrahigh-energy Particle Flux From Cosmic Strings*, *Phys. Lett. B* **246** (1990) 365.

[2] P. Bhattacharjee and G. Sigl, *Monopole annihilation and highest energy cosmic rays*, *Phys. Rev. D* **51** (1995) 4079 [astro-ph/9412053].

[3] G.A. Gusev, B.N. Lomonosov, K.M. Pichkhadze, N.G. Polukhina, V.A. Ryabov, T. Saito et al., *Detection of ultrahigh-energy cosmic rays and neutrinos by radio method using artificial lunar satellites*, *Cosmic Research* **44** (2006) 19.

[4] G.A. Askar'yan, *Excess negative charge of an electron-photon shower and its coherent radio emission*, *Zh. Eksp. Teor. Fiz.* **41** (1961) 616.

[5] R.D. Dagkesamansky and I.M. Zheleznykh, *Radio astronomy method for detecting neutrinos and other elementary particles of superhigh-energy*, *JETP Lett.* **50** (1989) 259.

[6] J. Alvarez-Muniz and E. Zas, *Cherenkov radio pulses from Eev neutrino interactions: The LPM effect*, *Phys. Lett. B* **411** (1997) 218 [astro-ph/9706064].

[7] C.W. James and R.J. Protheroe, *The sensitivity of the next generation of lunar cherenkov observations to uhe neutrinos and cosmic rays*, *Astroparticle Physics* **30** (2009) .

[8] O. Scholten, J. Bacelar, R. Braun, A.G. de Bruyn, H. Falcke, B. Stappers et al., *Optimal radio window for the detection of ultra-high-energy cosmic rays and neutrinos off the moon*, *Astropart. Phys.* **26** (2006) 219 [astro-ph/0508580].

[9] M.K. Shepard, R.A. Brackett and R.E. Arvidson, *Self-affine (fractal) topography: Surface parameterization and radar scattering*, *Journal of Geophysical Research: Planets* **100** (1995) 11709 [https://agupubs.onlinelibrary.wiley.com/doi/pdf/10.1029/95JE00664].

[10] T.M. McCollom and B.M. Jakosky, *Interpretation of planetary radar observations: the relationship between actual and inferred slope distributions*, *Journal of Geophysical Research: Planets* **98** (1993) 1173 [https://agupubs.onlinelibrary.wiley.com/doi/pdf/10.1029/92JE02544].

[11] K.G. Gayley, R.L. Mutel and T.R. Jaeger, *Analytic Aperture Calculation and Scaling Laws for Radio Detection of Lunar-Target UHE Neutrinos*, *Astrophys. J.* **706** (2009) 1556 [0904.3389].

[12] T.R. Jaeger, R.L. Mutel and K.G. Gayley, *Project RESUN, a radio EVLA search for UHE neutrinos*, *Astropart. Phys.* **34** (2010) 293 [0910.5949].